DOI 10.1515/aot-2013-0044 — Adv. Opt. Techn. 2014; 3(1): 103–111

Research Article

Astrid Bingel*, Kevin Füchsel, Norbert Kaiser and Andreas Tünnermann

ZnO:Al films prepared by inline DC magnetron sputtering

Abstract: Aluminum-doped zinc oxide (AZO) is one of the most promising transparent conductive oxide (TCO) materials that can substitute the high-quality but costly indium tin oxide (ITO). To ensure high-quality films as well as moderate production costs, inline DC magnetron sputtering was chosen to deposit thin AZO films. The influence of sputter gas pressure, substrate temperature, and film thickness on the electrical, optical, and structural properties was analyzed. The resistivity reaches a minimum of 1.3×10^{-5} Ωm at around 1 Pa for a substrate temperature of 90°C. A maximum conductivity was obtained by increasing the substrate temperature to 160°C. An annealing step after deposition led to a further decrease in resistivity to a value of 5.3×10^{-6} Ωm in a 200 nm thin film. At the same time, the optical performance could be improved. Additionally, simulations of the transmittance and reflectance spectra were carried out to compare carrier concentration and mobility determined by optical techniques with those from Hall measurements.

Keywords: aluminum-doped zinc oxide films; optimization of electrical and optical properties; postdeposition annealing; pulsed DC magnetron sputtering; transparent conductive oxides.

OCIS Codes: 310.1860 Deposition and fabrication; 310.3840 Materials and process characterization; 310.6860 Thin films, optical properties; 310.7005 Transparent conductive coatings.

***Corresponding author: Astrid Bingel,** Institute of Applied Physics, Abbe Center of Photonics, Friedrich-Schiller-Universität Jena, Max-Wien-Platz 1, 07743 Jena, Germany; and Fraunhofer Institute for Applied Optics and Precision Engineering, Albert-Einstein-Str. 7, 07745 Jena, Germany, e-mail: astrid.bingel@uni-jena.de

Kevin Füchsel and Norbert Kaiser: Fraunhofer Institute for Applied Optics and Precision Engineering, Albert-Einstein-Str. 7, 07745 Jena, Germany

Andreas Tünnermann: Institute of Applied Physics, Abbe Center of Photonics, Friedrich-Schiller-Universität Jena, Max-Wien-Platz 1, 07743 Jena, Germany; and Fraunhofer Institute for Applied Optics and Precision Engineering, Albert-Einstein-Str. 7, 07745 Jena, Germany

www.degruyter.com/aot

1 Introduction

Transparent conductive oxides (TCO) combine electrical conductivity with a high transparency in the visual spectral range. Therefore, they are especially suitable for transparent electrodes in flat panel displays [1] or thin film solar cells based on CIS or silicon [2–6]. Today, indium tin oxide (ITO) is commonly used on a commercialized production scale as TCO because of its excellent electrical and optical performance. However, ITO is both toxic and expensive because of its scarcity [7]. In recent years, aluminum-doped zinc oxide (AZO) turned out to be a high-quality competitor to ITO due to its lower material costs, nontoxicity, and its meanwhile comparable electrical and optical properties [8]. To deposit thin AZO films, a multiplicity of processes are possible such as pulsed laser deposition [9], chemical vapor deposition [10], spray pyrolysis [11], magnetron sputtering [12–14], or atomic layer deposition (ALD) [15].

Further fields of application for TCOs are so-called semiconductor-insulator-semiconductor (SIS) solar cells. Here, the challenge is to apply a low-cost deposition process, while simultaneously ensuring excellent electrical and optical characteristics. For these requirements, magnetron sputtering seems to be the most suitable process. Especially, DC sputtering from conductive ceramic targets has emerged as a potential solution to achieve relatively high deposition rates without a complicated process control as is necessary for reactive magnetron sputtering. Hence, for an efficient realization of our novel Nano-SIS solar cell concept, based on a nanostructured silicon surface [16], the deposition of the containing AZO layer should be done by pulsed DC magnetron sputtering from ceramic targets in an inline sputtering system.

This paper investigates the influence of the sputter gas pressure, substrate temperature, and vacuum annealing to the electrical, optical, and structural properties of thin ZnO:Al films on glass. The optical spectra are modeled with an extended Drude formula [17] to obtain plasma frequency and damping coefficient that can be compared to the Hall-measured carrier concentration N and mobility μ.

2 Experimental

ZnO:Al layers were deposited on glass substrates using pulsed DC magnetron sputtering in an MRC 903 inline magnetron sputtering system with a fixed sputter-pulse frequency of 100 kHz. We operated in dynamic deposition mode at a power density of P=3.3 W/cm² and P=4.4 W/cm², respectively.

The substrates were cleaned ultrasonically prior to the deposition and placed parallel to the target at a distance of 60 mm. The sputtering was carried out from a ceramic target with an alumina content of 2 wt%. Both in internal pretests and in literature, this was found to be the optimum target composition to produce low ohmic films (see, e.g., [12]).

After evacuating the process chamber to a base pressure of about 9×10^{-5} Pa, pure Argon was introduced by mass flow controllers. The substrate heating was realized by halogen lamps. Substrate temperatures from 65°C (only heat impact by sputtering) up to 260°C were investigated during the deposition process. However, the halogen lamps were mounted on an adjacent target station, meaning that there was only heat input available when the substrate holder passed the heating. Hence, the temperatures given are just mean values. Additionally, a two-step annealing after the deposition was investigated. First, the substrates were rapidly annealed within the load lock of the sputtering system by halogen lamps for approximately 7 min at temperatures up to 300°C. Second, the samples were treated in an external vacuum annealing furnace (*Systec*) for 2 h at 350°C.

X-ray diffraction was applied to determine the crystal structure of the thin films using a D5005 (*Bruker*) diffractometer. The surface morphology of the films was observed using a 'ΣIGMA' (*Carl Zeiss*) scanning electron microscope (SEM). The optical transmittance and reflectance spectra in the wavelength range of 250–2500 nm were measured with a PerkinElmer Lambda 950 spectrometer. The specific resistivity as well as the carrier concentration and carrier mobility was determined with a linear four-point probe and a Hall measurement system under van der Pauw configuration, respectively.

3 Results and discussions

3.1 Influence of sputter gas pressure

The influence of the sputter gas pressure on the resulting ZnO:Al film properties – especially electrical – is not discussed much in literature. The authors, who investigated this topic, partially gave different dependencies [13, 18–20]. Particularly, the pressure dependence for a dynamic deposition mode is rarely included. Only the authors of [20] compare the results for static and dynamic deposition where they report different behaviors when changing the deposition mode. Therefore, the pressure dependence for a dynamic deposition is investigated in detail in this section.

Figure 1 shows the specific resistivity as well as the carrier concentration and mobility of AZO films prepared at different working pressures ranging from 0.09 Pa to 1.7 Pa and a substrate temperature of 90°C. The film thickness was kept constant at around 200 nm in order to ensure the comparability of the results. The deposition was carried out in a pure argon atmosphere because pretests have shown that the addition of the lowest controllable flux of oxygen led to high resistivity in the range of 2×10^{-4} Ωm and high optical absorption losses of about 6% in the visual spectral range.

The argon sputtered films exhibit low resistivity in the range of 10^{-5} Ωm. This shows the successful substitutional doping with Al^{3+} ions because the electrical conductivity in AZO films is higher than that of pure ZnO films [21].

The specific resistivity decreases with increasing argon pressure and reaches a minimum value of 1.3×10^{-5} Ωm at around 1.1 Pa. At this point, the carrier concentration and mobility are 3.4×10^{20} cm^{-3} and 14.5 cm²/Vs, respectively. With a further increase in working pressure, the electrical parameters become slightly worse. This curve progression with a maximum conductivity between 1 Pa and 1.2 Pa could be observed for all temperatures meaning that the pressure dependency is independent of the substrate temperature.

To find an explanation for this behavior, the samples were investigated by SEM and X-ray diffraction. The results for different argon pressures are shown in Figures 2 and 3.

The SEM images show that the surface morphology changes with argon pressure. At a low argon pressure of 0.09 Pa, columns with very irregular formed cross sections can be observed. Additionally, there are speckles all over the surface that may be very small grains (<10 nm) or nucleus that are placed in between the larger grains. At the optimum working pressure of 1.1 Pa and even higher values, the grains appear rather round and denser packed. However, the determined mean grain size of about 50 nm did not change significantly with varying argon pressure. Although the grains exhibit the same diameter, it can be assumed that the structure that appears at 1.1 Pa is more suitable for an optimum carrier transport.

The XRD spectra of selected samples (Figure 3) all show a strong peak near 34.4°, which can be identified as the (002) peak of the ZnO hexagonal wurtzite structure. Furthermore, very weak diffraction peaks appear at 36.2° and 47°. They can be assigned to the (101) and (102) indices, respectively. The appearance of the strong (002) peak means that many of the crystallites building the film are orientated with their c-axis perpendicular to the substrate. To figure out the changes in crystal structure with increasing argon pressure, the (002) peaks were analyzed in detail. The results can be seen in Figure 3B. The dominant peak is located at angles that are smaller than the diffraction angle of bulk ZnO, 2θ=34.4°, which can be calculated

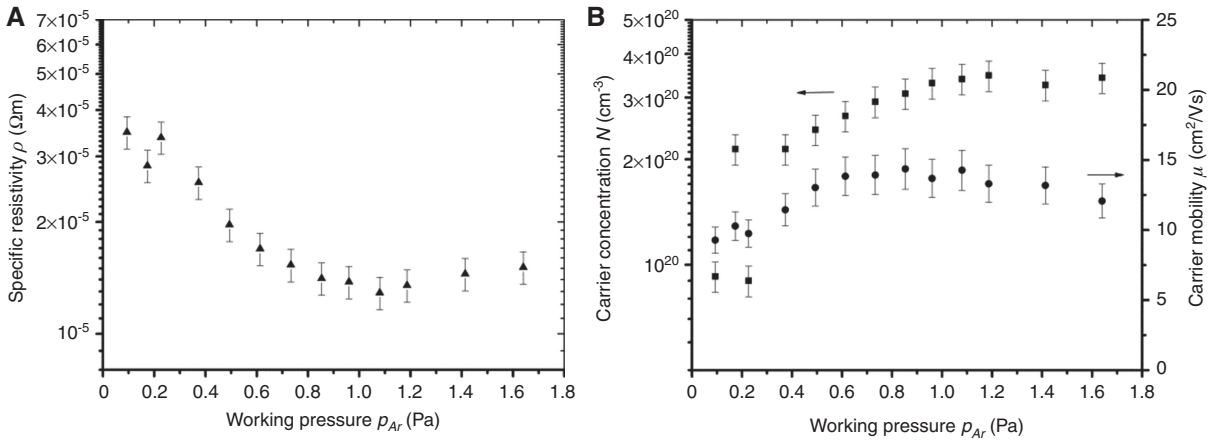

Figure 1 Specific resistivity (A) as well as the transport parameters (B) carrier concentration (■) and mobility (●) of 200-nm thin AZO films as a function of argon pressure. The temperature during the deposition was 90°C, and the power density applied to the substrate was 3.3 W/cm².

using the lattice parameter in the c-direction [21]. Values of $\theta<\theta_{bulk}$ result in a c-parameter larger than that of the bulk material suggesting macroscopic compressive stress [20]. Therefore, the stress within the layers is reduced with increasing sputter gas pressure because the diffraction angle approaches that of the undoped bulk material. The FWHM values of the (002) peaks are decreasing and remain nearly constant above the optimum working pressure of 1.1 Pa. This testifies to a reduction of microscopic stress, curing of defects, and an increase in grain size [20]. The width of the diffraction peak is a degree of structural quality of the films. That is a reason for the increase in mobility because the barriers for the carrier transport are reduced. Hence, the specific resistivity achieves its minimum at this point. Furthermore, one can assume that the stress relaxation is caused by an improved integration of Al^{3+} ions on zinc lattice sites [20]. Therefore, the doping is more effective, and the carrier concentration increases.

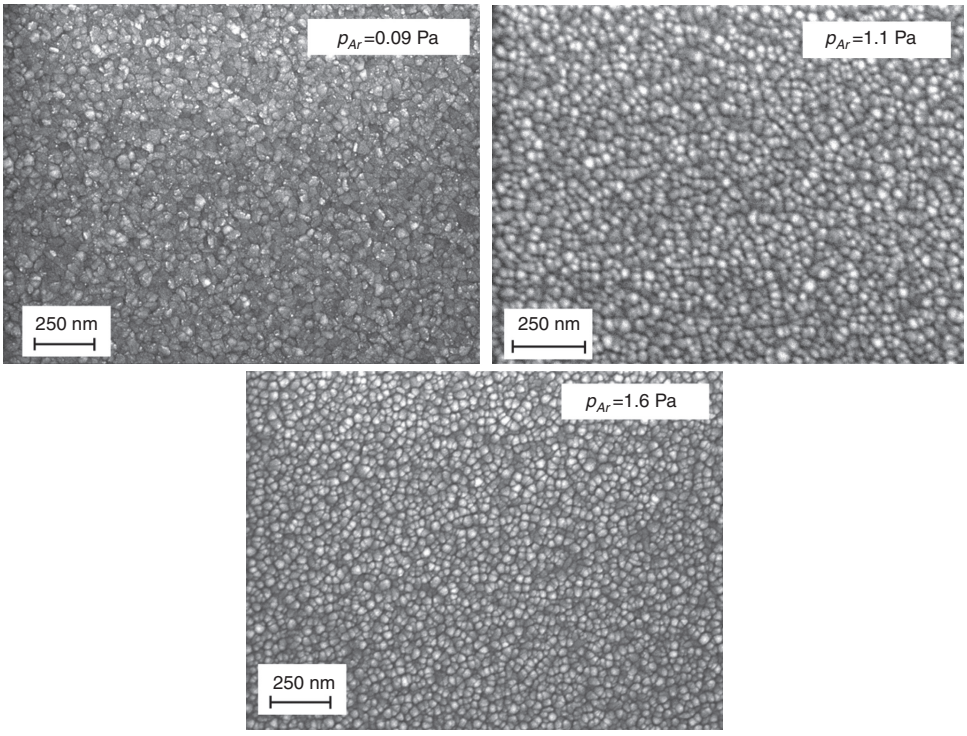

Figure 2 SEM images of ZnO:Al films deposited at different argon pressures at a substrate temperature of 90°C.

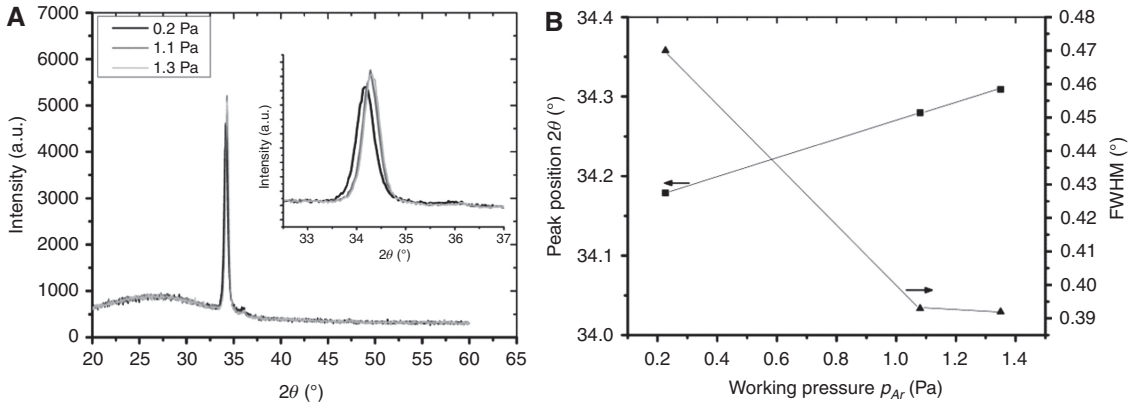

Figure 3 XRD spectra (A) as well as peak positions and FWHM of the (002) peak vs. p_{Ar} (B) for samples that were prepared at a substrate temperature of 90°C.

As mentioned before, the results that can be found in literature concerning this topic are slightly different from the curves presented here. For example, the authors of [13, 18–20] report on constant values of ρ over a wide range of argon pressure for films that are prepared in the static deposition mode. But especially Kluth et al. [20] investigated some changes when switching to dynamic deposition mode. They report decreasing resistivity with increasing pressure. Also, the values of 2θ and the FWHM show the same trend as can be seen in Figure 3.

In general, the conductivity got worse when changing from static to dynamic deposition, which can be explained by the processes taking place in the region of target erosion. It is has been reported numerously that the resulting resistivity in these areas is much higher than between the racetracks (see, e.g., [13, 22]). This results from the increased bombardment of the film with high energetic oxygen ions as well as neutral oxygen. Therefore, the crystalline quality of the films degrades. Now, in the dynamic mode, the substrate is moved under the target during the deposition. Therefore, the growing film can be understood as a multilayer stack one after another grown with the properties of the static print from the left to the right [20]. If the pressure in the vacuum chamber is increased, the mean free path of the atoms and ions, including the high energetic oxygen particles, is reduced. Hence, there is less bombardment, which improves the crystalline properties and becomes noticeable in the electrical parameters [13]. However, a further raise of argon pressure would lead to a thermalization of the sputtered particles and, therefore, a deterioration of the crystalline properties. Here, it can be seen that at a pressure above 1.4 Pa, the carrier mobility begins to drop. Additionally, Sato et al. account the decrease in N and μ with the rising pressure to an elevated oxidization [13].

3.2 Influence of substrate temperature

For a further improvement of electrical and optical parameters, the influence of the substrate temperature was studied. After investigating the sputter gas pressure in detail, the optimum value of p_{Ar} was found to be nearly constant at all temperatures. Therefore, an argon pressure of approximately 1.1 Pa was used for all following experiments. The substrate temperature was varied between 65°C (no substrate heating) and 260°C. The results concerning ρ, N, and μ for the 200 nm thin films are shown in Figure 4.

A minimum specific resistivity of 8.2×10^{-6} Ωm was found at a substrate temperature of 160°C. The related values for N and μ are 4.3×10^{20} cm^{-3} and 18.2 cm²/Vs, respectively. This improvement in conductivity was expected since a higher deposition temperature implies a higher mobility of the adatoms on the substrate surface to form a better crystalline structure. It also provides energy to activate more dopants, and an increased oxygen desorption is possible, which can lead to a higher N caused by oxygen vacancies as well as a reduction in carrier scattering at oxygen impurities that may be embedded into the grain boundaries. However, above this optimum temperature, the resistivity increases again. This is caused by a lowered mobility.

To investigate this drop in conductivity at higher temperatures, further film analysis was carried out. The surface morphology does not show any changes with substrate temperature, and also, the XRD spectra are not varying significantly (not shown here). Above a substrate temperature of 65°C, the (002) peak position remains nearly constant at (34.29±0.03)°, and its FHWM varies around (0.405±0.003)°.

Additionally, texture measurements were performed. This method is applied to verify if a preferred orientation

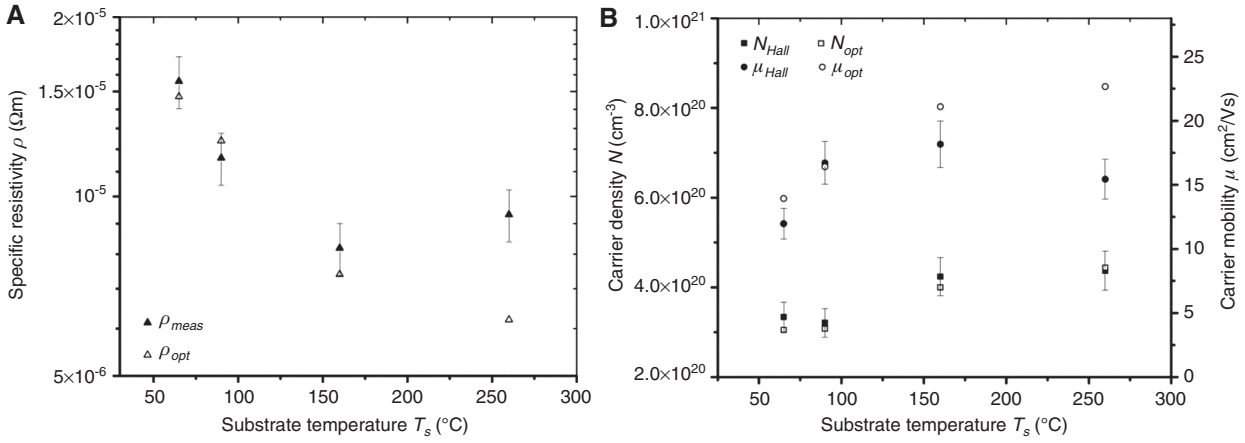

Figure 4 Electrical parameters ρ, N, and μ of 200-nm thin ZnO:Al films sputtered at p_{Ar}=1.1 Pa and P=4.4 W/cm² as a function of substrate temperature. In addition to the measured values, the data extracted from optical modeling are shown.

of the crystallites exists – here the (002) orientation. In general, the texture was not very distinctive. Only the sample prepared at 260°C showed slightly higher grade of texture.

Ellmer [23] stated that in thin TCO films, the maximum in conductivity complies with a maximum in texture because the scattering of the electrons induced by grain boundaries is lowest when all grains are oriented in the same direction. However, this could not be proven in our work because the film with a slightly higher grade of texture showed an increase in resistivity. Hence, the reason for the decrease in mobility at substrate temperatures above 160°C is not caused by the grain boundary scattering itself.

For a further investigation of this behavior, the electrically measured parameters were compared to optically determined values of carrier concentration N_{opt} and mobility μ_{opt}. For that purpose, the transmittance and reflectance spectra were fitted applying a multi-oscillator model [24]. The NIR spectral range of the resulting dielectric function was subsequently considered to obtain information about plasma frequency and mobility using an extended Drude model [17]. With an effective mass depending on the carrier concentration, the optical mobility μ_{opt} as well as carrier concentration N_{opt} could be calculated. A simplified procedural method with the Drude model can be found in an earlier publication [25]. The results can be seen in Figure 4 (open symbols). The agreement of carrier concentrations N_{Hall} and N_{opt} is very high. Also, the optical mobility μ_{opt} coincides with the Hall mobility for temperatures up to 160°C. However, for T_s=260°C, μ_{Hall} decreases, whereas μ_{opt} shows a further increase. Therefore, also ρ_{meas} and ρ_{opt} disagree at T_s=260°C. This may be caused due to the different excitation modes in Hall measurements and optical measurements. In the former case, the electrons are driven by a DC voltage, which let them pass also grain boundaries. In contrary, the high-frequency electrical field in the visible spectral range deflects the electrons only within the grains, and thus, any scattering mechanism at grain boundaries or at the edges of the grains cannot influence their motion. The theory that the grain boundaries, itself, act as the scattering mechanism could be disproved by a texture measurement. But nevertheless, it is possible that there are other scattering centers within the grain boundaries that constrain the carrier transport. For example, the segregation of Al_2O_3 or metal atoms within the grain boundaries is possible at higher temperatures [26, 27]. Although there is no proof for this hypothesis, it should be lined out that the behavior at high substrate temperatures originates within the grain boundaries because of the difference in Hall measured and optically determined mobility.

After the electrical parameters were discussed in detail, the optical properties of the ZnO:Al films will also be regarded. As a result of modeling the optical spectra with the multi-oscillator model, the spectral characteristics of the absorption and extinction coefficients were determined (Figure 5A, B). An increase in the free carrier absorption in the IR is observed when the substrate temperature rises. This is a consequence of the increasing conductivity. But it becomes apparent that the film prepared at T_s=260°C has a higher free carrier absorption, although the measured conductivity was lower than that of the sample deposited at T_s=160°C. This coincides with the results presented in Figure 4 where the optical measurements differ from the electrical.

The UV absorption (E>3 eV) that originates in the band-to-band excitation shows a shift of the absorption

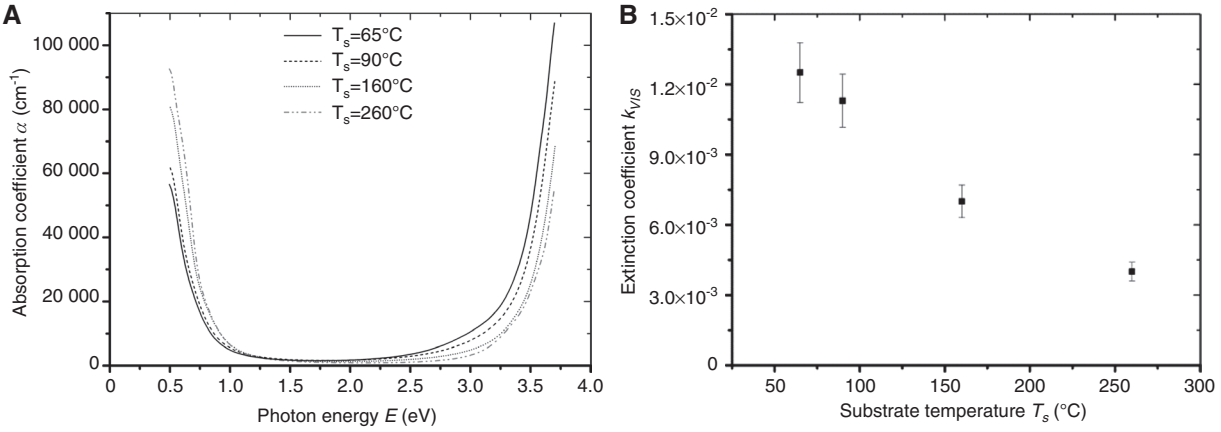

Figure 5 Absorption coefficient α determined by modeling the optical spectra (A) as well as the mean extinction coefficient k in the visual spectral range (B) for samples prepared at different substrate temperatures.

edge to higher energies with increasing temperature and carrier concentration, respectively. This behavior is well known for degenerated semiconductors as the Burstein-Moss Shift [28, 29].

To estimate the transparency of the films, the mean value of the extinction coefficient k in the visual spectral range (450–650 nm) was calculated. Figure 5B shows that the visual extinction coefficient k_{Vis} is lowered from 1.25×10^{-2} to 4×10^{-3} when the substrate temperature is increased to 260°C. This corresponds to mean transmittance values of 81% and 86% in the 200-nm thin films, respectively.

3.3 Improvement of ZnO:Al properties through annealing

The results of the previous section have shown that an improvement of electrical and optical properties of thin ZnO:Al films can be realized by a heat input to the layer. In literature, it is often reported on a reduction of specific resistivity by a heat treatment in vacuum [27, 30–32].

In this work, the deposition first was performed at optimum conditions, i.e., p_{Ar}=1.1 Pa and T_s=160°C. The subsequent annealing was implemented in a two-step process. First, the samples were irradiated by halogen lamps within the load lock of the sputtering system. This rapid thermal annealing was carried out at 2×10^{-4} Pa for 7 min, and the substrate surface reached a temperature of about 300°C. Afterwards, an annealing in an external vacuum furnace for 2 h at a temperature of 350°C and a pressure of 10^{-3} Pa followed.

Figure 6A shows the improvement of specific resistivity by the different heating steps. Here, samples with varying film thickness d were prepared to investigate also the thickness dependence of the conductivity as observed, e.g., in [12]. The drop of ρ with increasing thickness is mainly caused by a rising mobility (see Figure 6C), which originates from an improvement of structural quality and grain size.

The rectangular symbols represent the resistivity of the films prepared with optimum sputtering parameters that were investigated in Section 3 without additional annealing.

The first annealing step lowered the resistivity of a 200-nm thin film from 8.2×10^{-6} Ωm to 6×10^{-6} Ωm as can be seen in Figure 6A (circles). This is attributed to an increase in carrier concentration to 6×10^{20} cm^{-3}. On the other hand, the mobility remains almost constant (see Figure 6B and C).

Also the expected improvement in visual transparency occurred. By calculating the mean value of k in the visual spectral range, it turns out that a decrease from 7×10^{-3} (no annealing) to 4×10^{-3} takes place. This corresponds to a mean visual transmittance of 86.5% in a 200-nm thin film.

After this short but intensive annealing step, the samples were heat treated for 2 h in the external vacuum furnace at the conditions stated above. The results are also shown in Figure 6A (triangles). The 200-nm film exhibits a resistivity of 5.3×10^{-6} Ωm; however, this time, the improvement is caused by an increase in μ from 18.2 cm²/Vs to 20 cm²/Vs. In an 800-nm thick film, both the conductivity and mobility is even higher ($\rho=4\times10^{-6}$ Ωm, μ=27.5 cm²/Vs).

From these results, one can conclude that rapid thermal annealing step is able to increase the carrier concentration of the ZnO:Al films deposited in this work. This may be attributed to an activation of Al dopants as well as the oxygen desorption that elevates the contribution of

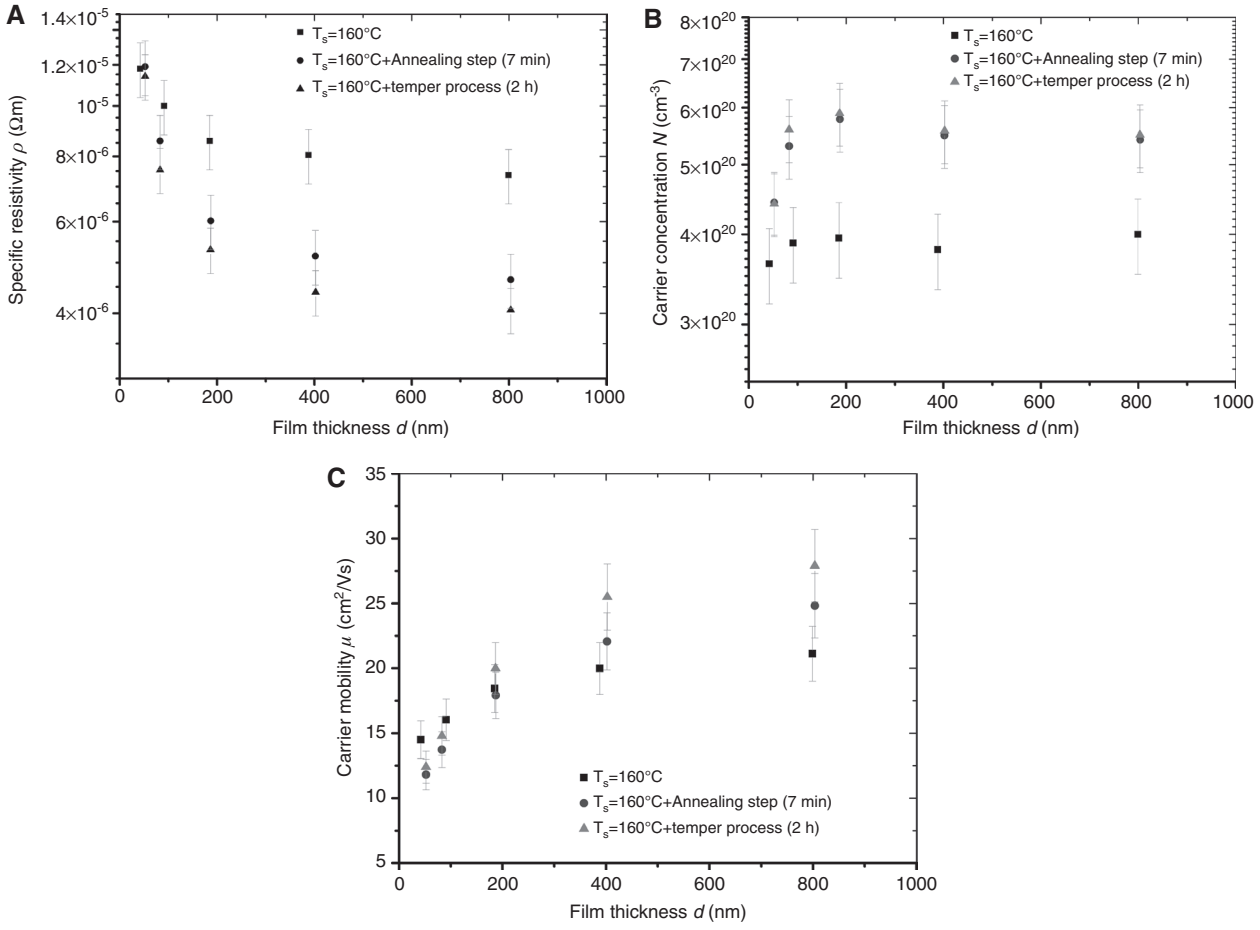

Figure 6 Improvement of specific resistivity by both different heating steps as well as an increasing film thickness (A) as well as the corresponding carrier concentration (B) and mobility (C).

oxygen vacancies to the free carrier density. On the contrary, a long time tempering process leads to a curing of defects and, therefore, an increase in carrier mobility.

4 Conclusion

Transparent and conductive aluminum-doped zinc oxide films have been prepared by DC magnetron sputtering from a ceramic target with 2 wt% Al_2O_3 content. The process was carried out in an inline sputtering system in dynamic mode.

A minimum resistivity of 1.3×10^{-5} Ωm was found at an optimized argon pressure of 1.1 Pa and a substrate temperature of 90°C. Variations in electrical conductivity also involve changes in film structure and may be related to a reduced bombardment with high energetic oxygen.

When increasing the substrate temperature up to 160°C, the resistivity reaches a minimum value of 8.2×10^{-6} Ωm, which is caused by an increase in mobility and carrier concentration. But a further temperature rise led to a lower mobility μ_{Hall} and, therefore, a higher resistivity. However, the values obtained for the mobility from modeling the optical spectra showed a different behavior. Therefore, it is expected that a scattering mechanism within the grain boundaries or at the edge of the grains plays an important role in AZO films grown at a substrate temperature above 160°C. The extinction coefficient in the visual spectral range k_{Vis} could be reduced by increasing the substrate temperature.

AZO films with a thickness of 200 nm grown at a substrate temperature of 160°C and subsequently annealed within the sputtering system or an external heating process reach a resistivity of 6×10^{-6} Ωm and 5.3×10^{-6} Ωm, respectively. The latter value corresponds to a mobility of 20 cm²/Vs and a carrier concentration of 5.9×10^{20} cm^{-3}. It was shown that a short and intensive annealing raises the carrier concentration, whereas the long-term tempering process improves the electron mobility. Also, a decrease of k_{Vis} from

7×10^{-3} (no annealing) to 4×10^{-3} takes place, which conforms to a visual transmittance of 86.5% in a 200-nm thin film.

Acknowledgments: This work was financially supported by the 'Novel-Optics' and 'ForMaT' funding program of the German Federal Ministry of Education and Research, under contract number 13N9669 and 03FO3292, respectively.

Received July 30, 2013; accepted October 2, 2013; previously published online November 14, 2013

References

[1] Y. Li, G. S. Tompa, S. Liang, C. Gorla, Y. Lu et al., J. Vac. Sci. Technol. A 15, 1063 (1997).
[2] B. Rech and H. Wagner, Appl. Phys. A: Mater. Sci. Process. 69, 155–167 (1999).
[3] U. Rau and H. W. Schock, Appl. Phys. A: Mater. Sci. Process. 69, 131–147 (1999).
[4] J. Müller, O. Kluth, S. Wieder, H. Siekmann, G. Schöpe, et al., Sol. Energy Mater. Sol. Cells 66, 275–281 (2001).
[5] B. Rech, O. Kluth, T. Repmann, T. Roschek, J. Springer, et al., Sol. Energy Mater. Sol. Cells 74, 439 (2002).
[6] T. Nakada, Y. Hirabayashi, T. Tokado, D. Ohmori and T. Mise, Sol. Energy 77, 739–747 (2004).
[7] D. Song, P. Widenborg, W. Chin and A. Aberle, Sol. Energ. Mat. Sol. C. 73, 1–20 (2002).
[8] T. Minami, Semicond. Sci. Technol. 20, 35 (2005).
[9] H. Agura, A. Suzuki, T. Matsushita, T. Aoki and M. Okuda, Thin Solid Films 445, 263–267 (2003).
[10] D. Lamb and S. Irvine, J. Cryst. Growth 273, 111 (2004).
[11] M. Miki-Yoshida, F. Paraduay-Delgado, Q. Estrada-López and E. Andrade, Thin Solid Films 376, 99–109 (2000).
[12] C. Agashe, O. Kluth, G. Schöpe, H. Siekmann, J. Hüpkes, et al., Thin Solid Films 442, 167–172 (2003).
[13] H. Sato, T. Minami and S. Takata, Thin Solid Films 220, 327–332 (1992).
[14] F. Ruske, A. Pflug, V. Sittinger, W. Werner, B. Szyszka, et al., Thin Solid Films 516, 4472–4477 (2008).
[15] M. Steglich, A. Bingel, G. Jia, F. Falk, Sol. Energ. Mat. Sol. C. 103, 62–68 (2012).
[16] K. Füchsel U. Schulz, N. Kaiser, T. Käsebier, E.-B. Kley, et al., Proc. SPIE 7725, 772502-8 (2010).
[17] D. Mergel and Z. Qiao, J. Phys. D: Appl. Phys. 35, 794–801 (2002).
[18] S. Bai and T. Tseng, J. Mater. Sci.-Mater. El. 20, 253–256 (2009).
[19] S. Rahmane, M. A. Djouadi, M.S. Aida, N. Barreau, B. Abdallah, et al., Thin Solid Films 519, 5–10 (2010).
[20] O. Kluth, G. Schöpe, B. Rech, R. Menner, M. Oertel, et al., Thin Solid Films 502, 311 (2006).
[21] Ü. Özgür, Y. I. Alivov, C. Lui, A. Teke, M. A. Reshichikov, et al., J. Appl. Phys. 98, 04103 1 (2005).
[22] Y. Imanishi, M. Taguchi, K. Onisawa, Thin Solid Films 518, 2945–2948 (2010).
[23] K. Ellmer, J. Phys. D: Appl. Phys. 33, R17–R32 (2000).
[24] O. Stenzel, S. Wilbrandt, K. Friedrich and N. Kaiser, Vak. Forsch. Prax. 21, 15–23 (2009).
[25] K. Füchsel, U. Schulz, N. Kaiser and A. Tünnermann, Appl. Optics 47, C297–C302 (2008).
[26] J. F. Chang and M. H. Hon, Thin Solid Films 386, 79–86 (2001).
[27] C. Guillén and J. Herrero, Vacuum 84, 924–929 (2010).
[28] E. Burstein, Phys. Rev. 93, 632–633 (1954).
[29] T. S. Moss, Proc. Phys. Soc. B 67, 775–782 (1954).
[30] G. Fang, D. Li and B. Yao, Vacuum 68, 363 (2003).
[31] M. Bouderbala, S. Hamzaoui, M. Adnane, T. Sahraoui and M. Zerdali, Thin Solid Films 517, 1572–1576 (2009).
[32] H.-J. Cho, S. U. Lee, B. Hong, Y. D. Shin, J. Y. Ju, et al., Thin Solid Films 518, 2941 (2010).

Astrid Bingel studied physics at the Friedrich-Schiller University in Jena and received her diploma in 2010. Since 2008, she is a research associate at the Fraunhofer Institute for Applied Optics and Precision Engineering (IOF) in Jena, and since 2011, she works on her PhD thesis at the IOF and Institute of Applied Physics in the field of transparent conductive oxides for photovoltaic and detector applications.

Kevin Füchsel studied Physics at the Friedrich-Schiller University (FSU) in Jena and received his diploma in 2007. His diploma thesis was on 'Low temperature deposition of indium tin oxide.' From 2008 to 2013, he worked on his PhD thesis with the title 'Nanostructured semiconductor-insulator-semiconductor solar cells.' Since 2008, he is a research associate and project leader at the Fraunhofer Institute for Applied Optics and Precision Engineering (IOF), and since 2011, he is a Junior Research Group Leader at the Institute of Applied Physics/FSU. In July 2013, he became the head of the Department of Strategy, Marketing, and Coordination at the Fraunhofer IOF.

Norbert Kaiser is a Professor for Physics and Technology of Thin Films at Ernst-Abbe-Technical University Jena. He heads the Optical Thin Film Department and is the Vice Director of the Fraunhofer Institute for Applied Optics and Precision Engineering in Jena.

Andreas Tünnermann received his diploma and PhD degrees in Physics from the University of Hannover in 1988 and 1992, respectively. In 1997, he received the habilitation. He was the head of the Department of Development at the Laser Zentrum Hannover from 1992 to 1997. In the beginning of 1998, he joined the Friedrich-Schiller University in Jena, Germany, as a Professor and Director of the Institute of Applied Physics. In 2003, he was appointed as the Director of the Fraunhofer Institute for Applied Optics and Precision Engineering IOF in Jena. His main research interests include scientific and technical aspects associated with the tailoring of light. Andreas Tünnermann is author of more than 400 papers in renowned international journals. He is a sought-after expert in optics and photonics industry. He is the founder and member of the board of directors of the industry-driven cluster OptoNet Jena, one of the most dynamic regional optic clusters in Europe. His research activities on applied quantum electronics have been awarded, e.g., with the Gottfried-Wilhelm-Leibniz-Award (2005). In 2013, he became a Fellow of SPIE.